Nonlinear control of a selective catalytic reduction unit for a bio-fueled cogeneration plant

Asadzadeh, Seyed Mohammad; Papageorgiou, Dimitrios; Andersen, Nils Axel

Published in:
IFAC-PapersOnLine

Link to article, DOI:
10.1016/j.ifacol.2023.10.1330

Publication date:
2023

Document Version
Publisher's PDF, also known as Version of record

Available online at www.sciencedirect.com

ScienceDirect

IFAC Papers Online CONFERENCE PAPER ARCHIVE

IFAC PapersOnLine 56-2 (2023) 3923–3929

Nonlinear control of a selective catalytic reduction unit for a bio-fueled cogeneration plant

Seyed Mohammad Asadzadeh * **Dimitrios Papageorgiou** *
Nils Axel Andersen *

* *Technical University of Denmark, Department of Electrical and Photonics Engineering, Elektrovej 326, 2800 Kgs Lyngby, Denmark (e-mail: semoasa,dimpa,nian@dtu.dk).*

Abstract: The paper puts forward a method for control of selective catalytic reduction (SCR) units. First, a dynamic model of SCR performance including heat transfer, ammonia adsorption, NOx reduction, and ammonia oxidation is developed. The model is then more simplified to only include medium time scale dynamics which can be shaped using control. The obtained model is utilised in the design of a nonlinear control strategy for the regulation of the NOx emissions in the system. A robust observer of the system state is developed and exploited for control design. Numerical simulations verify the effectiveness of the proposed control system.

Keywords: Selective catalytic reduction, cogeneration plant

1. INTRODUCTION

Small-scale cogeneration using biomass has the potential to help create energy systems in the future that are reliable, economical, and resilient to intermittent renewable sources. In the ongoing research project SmartCHP, a cogeneration plant prototype that runs on fast pyrolysis bio-oil (FPBO) fuel is being created. A hybrid diesel generator/flue gas burner/boiler system makes up the cogeneration plant. The oxygen concentration of engine exhaust gas is the only oxidizer for FPBO combustion in the burner. To ensure that the emissions CO, NOx, and PM are below acceptable limits, and to increase overall efficiency, an innovative flue gas cleaning is being developed and tested as well. This flue gas treatment is based on a commercially available SCR NOx reduction system which requires urea/ammonia as its reducing agent. The NOx emissions from both the diesel engine and burner/boiler are reduced by SCR placed downstream of the boiler. A complete SCR system includes urea injection device, hydrolysis of water-urea solution into gaseous ammonia, catalytic coated units, and NOx/NH3 sensors. For more on the cogeneration plant concept and its components see Asadzadeh and Andersen (2022b).

In SmartCHP, SCR is subject to the varying operations of its upstream components. For instance, when the diesel generator or the boiler is at a high load, the flue gas temperature may rise to temperatures that severely impede NOx reduction performance. The same NOx reduction performance degradation also happens with a cool converter when the plant operates at a low electrical and/or thermal load (Kwak et al. (2012)). Moreover, meeting new and increasingly stringent emissions legislation introduce new challenges on controlling an SCR system (Nebergall et al. (2005)).

A control-oriented SCR model typically exhibits significant non-linearities. This means the system behavior strongly depends on the operating point mainly determined by incoming flue gas characteristics (i.e., temperature, flow rate, and NOx content). Another significant source of non-linearity is the cross-sensitivity of NOx sensor to ammonia slip. In this study, it is assumed that an NH3 sensor is available downstream of SCR and this sensor is not sensitive to NOx. Therefore, NOx and NH3 measurements are available for control design.

SCR control strategies start with simple open-loop control where the ammonia injection is regulated as a function of estimated NOx input. Although open loop strategies are sufficient in some applications and simple to implement, they may overuse urea when NOx input is not so high (Willems et al. (2007)). They also can not compensate for input NOx measurement errors and fast NOx input transients (Chi (2009)). An SCR feedback controller has the advantage of reducing the effects of errors in estimating or measurement of SCR inputs, aging of the catalyst, and NH3 injector clogging (Song and Zhu (2002)). Model-based control design for SCR systems is a well-studied subject Skaf et al. (2014). Conventional controllers based on a nonlinear model of an SCR system combined with a PID controller are reported as an efficient control strategy (Herman et al. (2009)). Sliding mode controllers are also developed for ammonia coverage ratio in an SCR unit (Ma and Wang (2020)).

The majority of the reported methods in the literature focus on keeping the NOx emissions under a desired limit, without however emphasising on keeping a specific output profile that can respect the allowed emission limits but also consider reduced ammonia injection rates. This paper

⋆ Sponsor and financial support acknowledgment goes here. Paper titles should be written in uppercase and lowercase letters, not all uppercase.

10.1016/j.ifacol.2023.10.1330

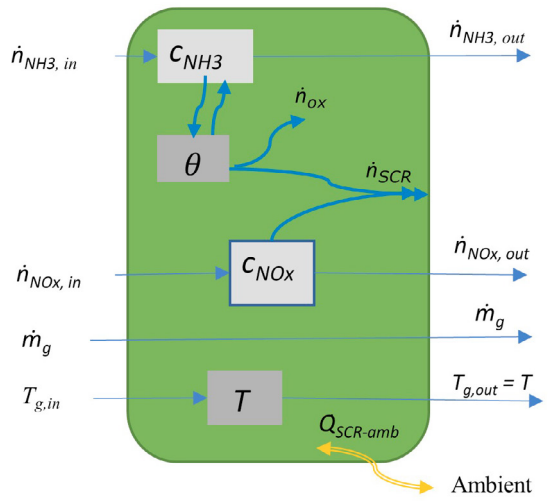

Fig. 1. Mass and heat flow in/out of SCR cell

contributes to the current body of knowledge by proposing a nonlinear feedback control strategy for the regulation of NOx emissions. The importance of such approach relates to the fact that the ability to track specific NOx profiles facilitates more consistent and monitorable system behaviour and better planning with respect to the levels of ammonia injection. Specifically, the contributions of the paper pertain to:

- development of a control-oriented model of a SCR system
- design of a robust estimator for the ammonia concentration that alleviates noise and numerical ill-posedness
- design and evaluation of a nonlinear feedback control scheme focusing on regulating the NOx emissions at a given output profile.

The remainder of the paper is structured as follows: Section 2 provides a description of the SCR system along with a control-oriented mathematical model. Section 3 details the nonlinear control design. Simulation results and evaluation of the proposed control architecture are presented in Section 4. Finally, conclusions are drawn in Section 5 along with a discussion on future work.

2. SCR SYSTEM DESCRIPTION AND MODELLING

The SCR gas treatment will require urea/ammonia as its reducing agent. A complete dynamic model of the SCR system includes the dynamics of urea solution injection device, the decomposition (hydrolysis) of water-urea solution into gaseous ammonia and CO_2, the reducing chemical reactions, and the dynamics of NOx/NH3 sensor. Here the focus is on the main dynamics of SCR which relate to its reducing chemical reactions.

Figure 1 shows a control-oriented representation of a SCR cell as well as its inputs-outputs. The chemical reactions included in this representation are adsorption and desorption of ammonia on the surface of the catalytic converter, the fast SCR reaction using equimolar amounts of NO and NO2, the main SCR reaction, and the oxidation of adsorbed ammonia from the surface of the catalyst.

The reaction for adsorption and desorption of ammonia on the catalyst reads

$$\mathrm{NH_3\,(gas)} \leftrightarrow \mathrm{NH_3\,(adsorbed)}$$

The forward reaction rate of adsorption (r_{ads}) is proportional with gaseous ammonia concentration (c_{NH3}) and the remaining capacity for adsorption $(1-\theta)$ on the surface of the catalyst

$$r_{\mathrm{ads}} = c_S S_C \alpha_{\mathrm{pr}} \sqrt{\frac{RT}{2\pi M_{\mathrm{NH3}}}} c_{\mathrm{NH3}}(1-\theta) \tag{1}$$

where θ is the scaled surface coverage with ammonia and is between [0,1], c_S is the concentration of active surface atoms per gas volume, S_C is the area of one mole of active surface atoms, α_{pr} is the sticking probability, M_{NH3} is molar mass of ammonia, and R is the universal gas constant, and T is the SCR temperature.

The backward reaction rate of desorption (r_{des}) is proportional with the used capacity for adsorption (θ)

$$r_{\mathrm{des}} = c_S k_{\mathrm{des}} \left(100 - b_0 - b_1 T - b_2 T^2\right) e^{\left(\frac{-E_{a,\mathrm{des}}}{RT}\right)} \theta \tag{2}$$

in which k_{des} is pre-exponential factor desorption, and $E_{a,des}$ is the activation energy of desorption.

The fast SCR reaction (SCR1) using equimolar amounts of NO and NO2 reads

$$4\mathrm{NH_3\,(ads)} + 2\mathrm{NO} + 2\mathrm{NO_2} \rightarrow 4N_2 + 6H_2O$$

The main SCR reaction (SCR2) with NO only reads

$$4\mathrm{NH_3\,(ads)} + 4\mathrm{NO} + O_2 \rightarrow 4N_2 + 6H_2O$$

An average rate of the fast and the main reactions, proportional to the available adsorbed ammonia and NOx concentrations, reads:

$$r_{\mathrm{SCR}} = c_S R k_{\mathrm{SCR}} \left(b_0 + b_1 T + b_2 T^2\right) e^{\left(\frac{-E_{a,\mathrm{SCR}}}{RT}\right)} \theta c_{\mathrm{NOx}} \tag{3}$$

where k_{SCR} is pre-exponential factor, and $E_{a,SCR}$ is an averaged activation energy of SCR reactions.

The oxidation of adsorbed ammonia reads

$$4\mathrm{NH_3\,(ads)} + 3O_2 \rightarrow 2N_2 + 6H_2O$$

with reaction rate

$$r_{\mathrm{ox}} = c_S k_{\mathrm{ox}} \left(100 - b_0 - b_1 T - b_2 T^2\right) e^{\left(\frac{-E_{a,\mathrm{ox}}}{RT}\right)} \theta \tag{4}$$

where k_{ox} is pre-exponential factor oxidation, and $E_{a,ox}$ is the activation energy of oxidation. Note that the concentration of O_2 does not enter the reaction rates as it is assumed to be sufficiently available in the flue gas. All the reaction rates are given in $\frac{\mathrm{mol}}{m^3 s}$.

The concentration of gases in the SCR may not be uniformly distributed. Therefore, their dynamics should be

expressed by partial differential equations. However, if the SCR is discretized into a few numbers of cells, arranged in series, then uniform distribution of gas concentration and homogeneous temperature in each cell is a justifiable (lumped parameter) assumption for acceptable approximation of the dynamics. With this approximation, a set of ODEs can represent the dynamics in each cell.

The ODE for the concentration of NOx reads

$$\dot{c}_{\mathrm{NOx}} = \frac{1}{V_{\mathrm{cell}}}\left[\dot{n}_{\mathrm{NOx,in}} - \dot{V} c_{\mathrm{NOx}}\right] - r_{\mathrm{SCR}} \tag{5}$$

where $V_{\mathrm{cell}} = \frac{V_c}{n_{\mathrm{cell}}}$ is volume of each cell and equals to SCR gas volume (V_c) divided by the number of cells (n_{cell}), and $\dot{V}$ is the volume flow of flue gas out of the SCR cell. The first two terms on the right-hand side of this ODE are the rate of NOx concentration change by gas inflow and outflow, and the last term is the rate of SCR reduction reactions.

The volume flow rate is

$$\dot{V} = \dot{m}_{\mathrm{g}}\,\frac{RT}{p_{\mathrm{amb}}} \tag{6}$$

where p_{amb} is SCR ambient pressure.

Similarly, the ODE for the concentration of NH3 is

$$\dot{c}_{\mathrm{NH3}} = \frac{1}{V_{\mathrm{cell}}}\left[\dot{n}_{\mathrm{NH3,in}} - \dot{V} c_{\mathrm{NH3}}\right] - r_{\mathrm{ads}} + r_{\mathrm{des}} \tag{7}$$

The dynamics of adsorbed ammonia on the surface of the catalyst is expressed by

$$c_S \dot{\theta} = r_{\mathrm{ads}} - r_{\mathrm{des}} - r_{\mathrm{SCR}} - r_{\mathrm{ox}} \tag{8}$$

The SCR cell and its housing are a thermal reservoir, and its temperature dynamics is expressed by

$$C_{\mathrm{cell}}\dot{T} = c_{p,g}\ \dot{m}_{g,in}\left(T_{g,in} - T\right) - \alpha_c A_c \left(T - T_{\mathrm{amb}}\right) \tag{9}$$

where specific heat capacity of flue gas at constant pressure is $c_{p,g}$ and $C_{\mathrm{cell}} = c_{p,SCR} m_{\mathrm{cell}}$ is thermal capacity of SCR cell, with specific heat capacity $c_{p,SCR}$ and mass $m_{\mathrm{cell}} = \frac{m_c}{n_{\mathrm{cell}}}$, and α_c and A_c are coefficient and area for heat transfer by convection from SCR cell to its ambient. For the sake of brevity, the interested reader is referred to Asadzadeh and Andersen (2022a) where the model parameters are defined and identified with respect to published experimental data of two SCR units (Kwak et al. (2012)).

2.1 Simplified control-oriented model

The following assumptions have contributed to simplification of the SCR dynamic model in order to facilitate efficient control design:

- Ammonia and NOx concentration dynamics are much faster than that of ammonia coverage, hence they are considered at their steady state and are represented by static functions. This means from equations (5) and (7) the steady state concentrations are calculated as in equations (14) and (15)
- Reaction enthalpies and their thermal effects are neglected

Let us define temperature dependent functions $\alpha_{\cdot}(T)$ as:

$$\begin{aligned}
&\alpha_{\mathrm{ads}}(T) = c_S S_C \alpha_{\mathrm{pr}} \sqrt{\frac{RT}{2\pi M_{\mathrm{NH3}}}} \\
&\alpha_{\mathrm{des}}(T) = c_S k_{\mathrm{des}} \left(100 - b_0 - b_1 T - b_2 T^2\right) e^{\left(\frac{-E_{a,\mathrm{des}}}{RT}\right)} \\
&\alpha_{\mathrm{SCR}}(T) = c_S R k_{\mathrm{SCR}} \left(b_0 + b_1 T + b_2 T^2\right) e^{\left(\frac{-E_{a,\mathrm{SCR}}}{RT}\right)} \\
&\alpha_{\mathrm{ox}}(T) = c_S k_{\mathrm{ox}} \left(100 - b_0 - b_1 T - b_2 T^2\right) e^{\left(\frac{-E_{a,\mathrm{ox}}}{RT}\right)} \\
&\alpha_0 = \frac{R}{p_{amb}}, \alpha_1 = \frac{1}{V_{\mathrm{cell}}}
\end{aligned} \tag{10}$$

A compact form for the dynamics of adsorbed ammonia on the surface of the catalyst reads:

$$\dot{\theta} = f_\theta(t,\theta) + g_\theta(t,\theta)u \tag{11}$$

with $f_\theta(t,\theta) < 0$ and $g_\theta(t,\theta) > 0$ defined as

$$\begin{aligned}
f_\theta(t,\theta) \triangleq -\frac{1}{c_S}\Bigg\{&\alpha_{\mathrm{des}}(T)\,\frac{\alpha_0\alpha_1\dot{m}_g T}{\alpha_0\alpha_1\dot{m}_g T + \alpha_{\mathrm{ads}}(T)(1-\theta)} \\
&+\alpha_{\mathrm{ox}}(T) + \frac{\alpha_1\alpha_{\mathrm{SCR}}(T)}{\alpha_0\alpha_1\dot{m}_g T + \alpha_{\mathrm{SCR}}(T)\,\theta}\dot{n}_{NOX,in}\Bigg\}\theta
\end{aligned} \tag{12}$$

$$g_\theta(t,\theta) \triangleq \frac{1}{c_S}\left\{\frac{\alpha_1\alpha_{\mathrm{ads}}(T)(1-\theta)}{\alpha_0\alpha_1\dot{m}_g T + \alpha_{\mathrm{ads}}(T)(1-\theta)}\right\} \tag{13}$$

and where $u \triangleq \dot{n}_{\mathrm{NH3,in}}$ is the control input, $\dot{n}_{\mathrm{NOX,in}}$, T, $\dot{m}_g$ are time-varying measured inputs and $\theta \in (0,1)$ is the unmeasured state.

The objective of the control design is to keep NOx and NH3 concentrations downstream of the plant below their legally acceptable limits. These are measured outputs given by:

$$c_{\mathrm{NH3,out}} = \frac{\alpha_1\dot{n}_{\mathrm{NH3,in}} + \alpha_{\mathrm{des}}(T)\,\theta}{\alpha_0\alpha_1\dot{m}_g T + \alpha_{\mathrm{ads}}(T)(1-\theta)} \tag{14}$$

$$c_{\mathrm{NOx,out}} = \frac{\alpha_1\dot{n}_{\mathrm{NOX,in}}}{\alpha_0\alpha_1\dot{m}_g T + \alpha_{\mathrm{SCR}}(T)\,\theta} \tag{15}$$

3. CONTROL DESIGN

3.1 Estimation of θ

Knowledge of θ is necessary for all the subsequent control designs. Direct calculation based on the nonlinear mappings in either of (14) or (15) introduces unwanted effects of noise and numerical ill-posedness depending on the profile of $c_{\mathrm{NH3,out}}$ or $c_{\mathrm{NOx,out}}$, respectively. A smoother estimation of θ will be instead pursued by dynamically inverting the mapping in Equation (15) with respect to θ. Define

$$\phi(t,\theta) \triangleq \frac{\alpha_1\dot{n}_{NOX,in}}{\alpha_0\alpha_1\dot{m}_g T + \alpha_{SCR}(T)\theta} \tag{16}$$

Then an estimation law for θ is

$$\dot{\hat{\theta}} = \mathrm{Proj}\left[\hat{\theta}, \gamma\mu(t,\hat{\theta})\left(\phi(t,\theta) - \phi(t,\hat{\theta})\right)\right], \tag{17}$$

where $\hat{\theta}$ is an estimate of θ, $\gamma > 0$ is the adaptation gain and the projection operator Proj[·] is defined in Appendix A. The estimation law in (17) is very similar to conventional gradient decent-type laws used in parameter estimation and adaptive control problems with one significant difference: the gain is scaled by the function $\mu(\hat{\theta})$ which is a design degree of freedom. It has been shown (Grip et al., 2010) that the adaptive law (17) guarantees exponential estimation of the parameter θ, provided that the function $\mu(\hat{\theta})$ is designed such that it satisfies the following property:

Property 1. For any pair $(\theta_1, \theta_2) \in (0,1) \times (0,1)$ it holds

$$\mu(\theta_1)\frac{\partial \phi}{\partial \theta}(t,\theta_2) + \mu(\theta_2)\frac{\partial \phi}{\partial \theta}(t,\theta_1) \geq 2\sigma(t) \tag{18}$$

where $\sigma : \mathbb{R}_{>0} \to \mathbb{R}_{>0}$ is a positive definite scalar function that satisfies

$$|\phi(t,\theta) - \phi(t,\hat{\theta})| \leq L\sqrt{\sigma(t)}|\tilde{\theta}| \tag{19}$$

$\forall t \geq 0$ and $L > 0$.

Then the remaining steps in the design of the estimator is to select an appropriate $\mu(\theta)$ function.

Proposition 1. The function $\mu(\theta) \triangleq -\theta$ satisfies Property 1.

Proof. Indeed for $\mu(\theta) = -\theta$ and for $0 < \theta_{min} \leq \theta \leq \theta_{max} < 1$ one obtains

$$\mu(\theta_1)\frac{\partial \phi}{\partial \theta}(t,\theta_2) + \mu(\theta_2)\frac{\partial \phi}{\partial \theta}(t,\theta_1) =$$

$$\frac{\theta_1 \alpha_1 \dot{m}_{NOX,in} \alpha_{SCR}(T)}{\left(\alpha_0\alpha_1\dot{m}_g T + \alpha_{SCR}(T)\theta_2\right)^2} + \frac{\theta_2 \alpha_1 \dot{m}_{NOX,in} \alpha_{SCR}(T)}{\left(\alpha_0\alpha_1\dot{m}_g T + \alpha_{SCR}(T)\theta_1\right)^2} \geq$$

$$2\frac{\alpha_1 \dot{m}_{NOX,in} \alpha_{SCR}(T)}{\left(\alpha_0\alpha_1\dot{m}_g T + \alpha_{SCR}(T)\theta_{max}\right)^2}\theta_{min} \triangleq 2\sigma(t) > 0$$

Moreover, since

$$\left|\frac{\partial \phi}{\partial \theta}(t,\theta)\right| = \frac{\alpha_1 \dot{m}_{NOX,in} \alpha_{SCR}(T)}{\left(\alpha_0\alpha_1\dot{m}_g T + \alpha_{SCR}(T)\theta\right)^2}$$

is bounded $\forall \theta \in (0,1)$ and $\forall t \geq 0$, $\phi(t,\theta)$ is globally Lipschitz in θ. Therefore, $\exists L_0 > 0$ such that

$$|\phi(t,\theta) - \phi(t,\hat{\theta})| \leq L_0|\tilde{\theta}| = L_0\frac{\sqrt{\sigma(t)}}{\sqrt{\sigma(t)}}\tilde{\theta} \leq L\sqrt{\sigma(t)}|\tilde{\theta}| \tag{20}$$

with $L \triangleq \dfrac{L_0}{\min\limits_t \sqrt{\sigma(t)}}$, which completes the proof. ■

Finally, whenever $\dot{m}_{NOX,in} > 0$, i.e. whenever the engine is operating, $\sigma(t) > 0 \Rightarrow \int_t^{t+T}\sigma(\tau)d\tau \geq \int_t^{t+T}\min\limits_t \sqrt{\sigma(\tau)}d\tau = \min\limits_t \sqrt{\sigma(t)}T > 0$, $\forall t$ and for some $T > 0$. This corresponds to the standard persistence of excitation condition required for parameter estimation. Since Property 1 is satisfied and according to (Grip et al., 2010), the estimation error $\tilde{\theta} \triangleq \theta - \hat{\theta}$ exponentially converges to the origin in absence of any perturbations and for $\dot{\theta} = 0$. Since in general θ is not constant, the estimation error dynamics is perturbed by $\dot{\theta}$, which is bounded considering Equation (11). In this case it has been shown (Papageorgiou et al., 2018) that estimation error trajectories are uniformly globally ultimately bounded (UGUB). Moreover, the ultimate bound is proportional to the ratio of the perturbation bound over the adaptation gain.

Remark 1. In terms of application of the estimator, this means that the adaptation gain γ can be selected large enough compared to the maximum ammonia absorption rate $|\dot{\theta}|$, such that the bound on the estimation error $\sup\limits_t |\tilde{\theta}(t)|$ is sufficiently small.

3.2 Nonlinear feedback control of SCR

The objective is to control the output $c_{\mathrm{NOx,out}}$ so that it tracks a known smooth output profile signal $r(t)$ that conforms with the permissible limits. It is assumed that the derivatives of such a signal are available from a trajectory planner. Alternatively, the output can be regulated to a constant setpoint well below the NOx emission limits to allow for some deviation. Define $y \triangleq c_{\mathrm{NOx,out}}$. The regulation error $e \triangleq y - r$ dynamics reads

$$\dot{e} = \dot{y} = f(t,\theta) + g(t,\theta)u - \dot{r} \tag{21}$$

with

$$f(t,\theta) \triangleq \alpha_1 \left\{ \frac{\ddot{n}_{\mathrm{NOX,in}}(\alpha_0\alpha_1\dot{m}_g T + \alpha_{SCR}(T)\theta)}{\left(\alpha_0\alpha_1\dot{m}_g T + \alpha_{\mathrm{SCR}}(T)\theta\right)^2} \right.$$
$$- \frac{\dot{n}_{\mathrm{NOX,in}}\left[\alpha_0\alpha_1\left(\ddot{m}_g T + \dot{m}_g\dot{T}\right) + \dot{\alpha}_{\mathrm{SCR}}(T)\theta\right]}{\left(\alpha_0\alpha_1\dot{m}_g T + \alpha_{\mathrm{SCR}}(T)\theta\right)^2}$$
$$\left. - \frac{\dot{n}_{\mathrm{NOX,in}}}{\left(\alpha_0\alpha_1\dot{m}_g T + \alpha_{\mathrm{SCR}}(T)\theta\right)^2} f_\theta(t,\theta) \right\} \tag{22}$$

$$g(t,\theta) \triangleq -\frac{\alpha_1\dot{n}_{\mathrm{NOX,in}}}{\left(\alpha_0\alpha_1\dot{m}_g T + \alpha_{\mathrm{SCR}}(T)\theta\right)^2} g_\theta(t,\theta) \tag{23}$$

Since $\dot{n}_{\mathrm{NOX,in}}, \alpha_{SCR}(T) \neq 0$ and $g_\theta(t,\theta) > 0$ for all $(t,\theta) \in \mathbb{R} \times (0,1)$, the system in (21) is controllable. The signals $\ddot{m}_g, \ddot{n}_{\mathrm{NOX,in}}$ are not available from measurements and have to be estimated via robust differentiation of the signals $\dot{m}_g, \dot{n}_{\mathrm{NOX,in}}$. Moreover, θ is available through its estimate $\hat{theta}$. These imply that evaluating the functions f, g defined (22), (23) with known signals introduces bounded perturbations in the considered system dynamics. Additional perturbations are introduced due to parametric uncertainty. Let $\hat{f}(t,\hat{\theta}), \hat{g}(t,\hat{\theta}) \neq 0$ be an evaluation of f, g where all required derivatives are estimated and $\hat{\theta}$ has been used instead of the real value of ammonia absorption rate. The real dynamics of the regulation error then reads:

$$\dot{e} = \hat{f}(t,\hat{\theta}) + \underbrace{\left[f(t,\theta) - \hat{f}(t,\hat{\theta})\right]}_{\tilde{f}(t,\theta,\hat{\theta})} - \dot{r}$$
$$+ \hat{g}(t,\hat{\theta})u + \underbrace{\left[g(t,\theta) - \hat{g}(t,\hat{\theta})\right]}_{\tilde{g}(t,\theta,\hat{\theta})} u$$
$$= \hat{f}(t,\hat{\theta}) + \hat{g}(t,\hat{\theta})u + \underbrace{\tilde{f}(t,\theta,\hat{\theta}) + \tilde{g}(t,\theta,\hat{\theta})u}_{d(t,\theta,\hat{\theta})} + \dot{r} \ .$$

Remark 2. The time argument in the functions f_θ, g_θ, f, g and d abbreviates the explicit dependence of these functions in known bounded time-varying signals, such as $\dot{n}_{\mathrm{NOX,in}}, \dot{m}_g$ etc.

Under the control law

$$u = \frac{1}{\hat{g}(t,\hat{\theta})}\left[-\hat{f}(t,\hat{\theta}) - ke + \dot{r}\right] \tag{24}$$

where $k > 0$, the closed-loop error dynamics are written as

$$\dot{e} = -ke + d(t, \theta, \hat{\theta}) \tag{25}$$

Assumption 1. The perturbation $d(t, \theta, \hat{\theta})$ is uniformly bounded, i.e. $\exists \Delta > 0$ such that $|d(t, \theta, \hat{\theta})| < \Delta$, $\forall t \geq 0$.

This assumption is based on the fact that the perturbation d can be seen as a function of all possible parametric and estimation errors, which here are abbreviated with the vector $\boldsymbol{\delta p}$ (e.g $\tilde{\theta}$ and the differences between real $\ddot{n}_{\mathrm{NOX,in}}$, $\ddot{m}_g$ etc. from their estimated values are components of $\boldsymbol{\delta p}$). It is also a function of the state $\theta \in (0, 1)$ and of the input $u \in [0, u_{max}]$. In fact f, g are Lipschitz in all of its arguments since their gradients are bounded for bounded signals. Therefore, $\exists L_f, L_g > 0$ such that

$$|d| < L_f \left\| \begin{matrix} \boldsymbol{\delta p} \\ \theta \end{matrix} \right\| + L_g \left\| \begin{matrix} \boldsymbol{\delta p} \\ \theta \\ u \end{matrix} \right\| \leq L_f \Delta_1 + L_g \Delta_2 \triangleq \Delta$$

where $\Delta_1, \Delta_2 > 0$ are bounds for the norms of the two vectors in the above inequality.

Proposition 2. Under Assumption 1, the trajectories of the closed-loop system (25) are UGUB with ultimate bound inversely proportional to the controller gain k.

Proof. Consider the smooth, positive-definite, decrescent and radially unbounded Lyapunov function candidate defined as $V(e) \triangleq \frac{1}{2}e^2$. Its time-derivative along the trajectories of (25) is

$$\dot{V} = -ke^2 + ed \leq -ke^2 + |e|\Delta = -(1-\lambda)e^2 + |e|\left(-\lambda k|e| + \Delta\right) \leq -(1-\lambda)e^2, \ \forall |e| > \frac{1}{k}\frac{\Delta}{\lambda}$$

Then the closed-loop system trajectories are UGUB (Khalil, 2002) with the ultimate bound being inversely proportional to the controller gain. ■

3.3 Conventional control of SCR

The performance of the designed non-linear feedback controller is compared with a benchmark conventional controller from the literature (Schär (2003)). The design of this controller is based on a constant ratio $C = \frac{c_{NH3,out}}{c_{NOx,out}}$, when ammonia slip is allowed to reach a maximum of 15 ppm. Substituting output concentrations from (14) and (15) will give control input

$$u = \frac{G(t, \hat{\theta})}{C}\dot{n}_{\mathrm{NOX,in}} - \frac{\alpha_{des}(T)}{\alpha_1}\hat{\theta} \tag{26}$$

with $G(t, \theta) = \dfrac{\alpha_1 \dot{n}_{\mathrm{NH3,in}} + \alpha_{\mathrm{des}}(T)\,\theta}{\alpha_0 \alpha_1 \dot{m}_g T + \alpha_{\mathrm{SCR}}(T)\,\theta}$

Remark 3. It should be noted that the control law in (26) is not strictly feed-forward since it uses feedback from the estimated ammonia absorption. However, it is referred to as "feed-froward" in the literature in the sense that no feedback of the regulation error e is used. In a strict feed-forward implementation, a map-based ammonia absorption estimation would be used, where ammonia absorption is a function of flue gas volume flow and temperature. Here, to have a fair comparison, the estimated ammonia absorption from the designed observer is also available to the conventional controller.

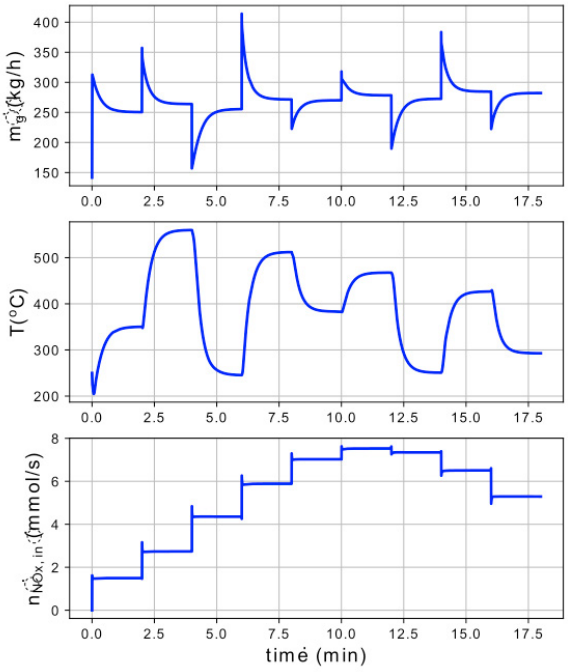

Fig. 2. Simulation scenario - input flue gas characteristics

4. SIMULATION RESULTS

The proposed control strategy is evaluated in a simulation scenario, where the SCR system is simulated in response to 9 steps of 5kW in the upstream diesel generator load (i.e., from low-load 5kW to high-load 45kW). Each step lasts for two minutes. This is combined with on-off periods of the burner which is located between the diesel generator and the SCR unit. The resulting input flue gas temperature, flow rate, and NOx formation are shown in Figure 2. The proposed control strategy is also compared with the conventional controller in section 3.3. For a fair comparison, both the proposed non-linear controller (NLC) and the conventional controller are tuned for their satisfactory and comparable performance, i.e., both use the same total amount of urea injection, as their available resource.

Figure 3 shows ammonia concentration and its estimations. The observer shows a robust and acceptable estimation of θ with quick convergence.

Figure 4 shows NOx emission concentration downstream of the SCR unit. For cogeneration applications in Europe, the allowable NOx emission limit is 180 mg/m^3. The NLC controller is set to regulate NOx output at 150 mg/m^3. The NLC controller shows better NOx reduction performance for the case of a cooler converter, which naturally entails considerable degradation of NOx reduction performance. Such an event happens in the third simulation step, between minutes 4-6 in Figure 4. The proposed NLC controller is able to regulate NOx emission at a certain desirable level unless the natural limitation of the converter does not allow for maximum NOx reduction, e.g., at very low or very high temperatures.

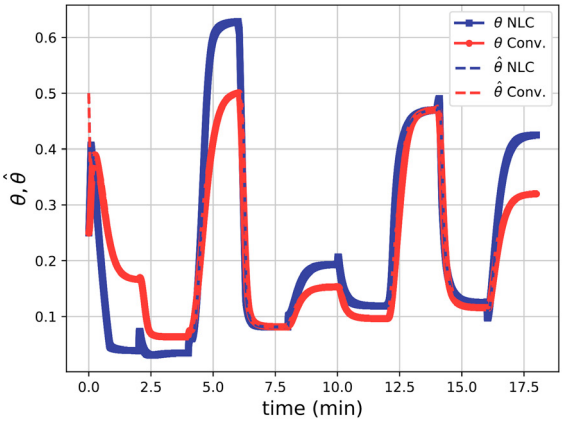

Fig. 3. Robust estimation of θ

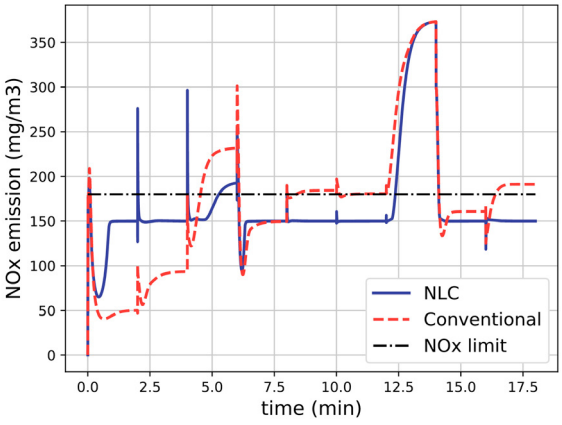

Fig. 4. Comparison of NOx emissions for the two control strategies

Figure 5 compares ammonia slip downstream of the SCR unit. Normally, there is a trade-off between NH3 slip and NOx removal. In this respect, NLC controller achieves higher NOx removal at the expense of more NH3 slip. But it is important for a control design to utilize such trade-off to achieve better overall performance. As shown in Table 1, the NLC controller achieves an average of 2 mg/m^3 lower NOx emission, compared to the conventional controller, at the expense of 0.7 *ppm* more NH3 slip, however the average NOx emissions that exceed the acceptable level is significantly lower for the NLC controller, i.e., 41 against 106 mg/m^3.

Table 1. Performance comparison of the control strategies

Controller	Average NH3 injection (ppm)	Average NH3 slip (ppm)	Average NOx emission (mg/m^3)	Sum NOx above limit (mg/m^3)
Conv.	1269	10.6	169	106
NLC	1269	11.3	167	41

The ammonia injection profile of the two controllers looks similar. An important difference is when the NOx emission

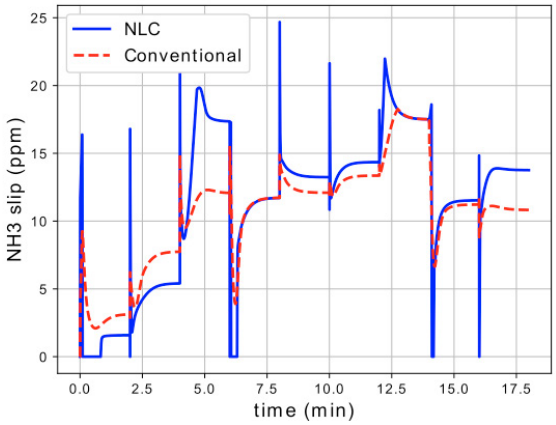

Fig. 5. Comparison of ammonia slip for the two control strategies

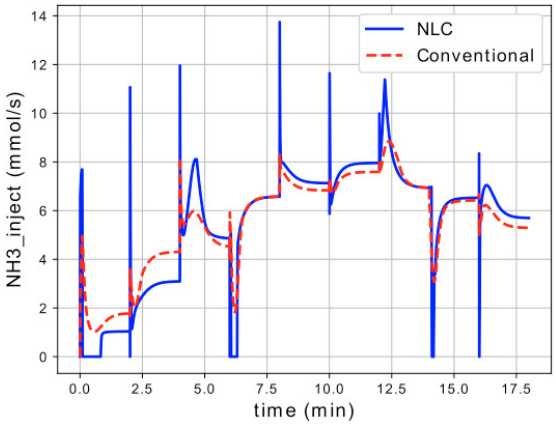

Fig. 6. Control input profiles for the two control strategies

is well below the acceptable limit, the NLC controller reduces the amount of injection to maintain NH3 slip at a lower level.

5. CONCLUSION

This study proposed a non-linear strategy for feedback control of an SCR unit. The design was based on a simplified control-oriented model of the SCR unit. The performance of the proposed control strategy was compared with a conventional good-performing open loop controller from the literature. A robust observer for the ammonia coverage was devised and used for state estimation for both controllers. The potential and advantages of the proposed controller were discussed. Closed-loop non-linear control may not be required to enhance nominal NOx removal performance. However, it shows potential to be tuned for regulating NOx emission close to the legally acceptable limits, thus enhancing compliance with regulations at a wide operating range of the cogeneration plant while maintaining minimal NH3 slip.

ACKNOWLEDGEMENTS

The SmartCHP project has received funding from the European Union's Horizon 2020 Research and Innovation programme under Grant Agreement No. 815259. The authors would like to thank the SmartCHP project partners for the provision of experimental data.

REFERENCES

Asadzadeh, S.M. and Andersen, N.A. (2022a). Model-based fault diagnosis of selective catalytic reduction for a smart cogeneration plant running on fast pyrolysis bio-oil. *IFAC-PapersOnLine*, 55(6), 427–432.

Asadzadeh, S.M. and Andersen, N.A. (2022b). A predictive dynamic model of a smart cogeneration plant fuelled with fast pyrolysis bio-oil. *J.sustain. dev. energy water environ. syst.*, 10(4), 1–20. doi: https://doi.org/10.13044/j.sdewes.d10.0430.

Chi, J.N. (2009). Control challenges for optimal nox conversion efficiency from scr aftertreatment systems. Technical report, SAE Technical Paper.

Grip, H.F., Johansen, T.A., Imsland, L., and Kaasa, G.o. (2010). Parameter estimation and compensation in systems with nonlinearly parameterized perturbations. *Automatica*, 46(1), 19–28. doi: 10.1016/j.automatica.2009.10.013.

Herman, A., Wu, M.C., Cabush, D., and Shost, M. (2009). Model based control of scr dosing and obd strategies with feedback from nh3 sensors. *SAE International Journal of Fuels and Lubricants*, 2(1), 375–385.

Khalil, H.K. (2002). Nonlinear systems third edition. *Patience Hall*, 115.

Krstic, M., Kanellakopoulos, I., and Kokotovic, P.V. (1995). *Nonlinear and Adaptive Control Design*. Wiley-Interscience, 1 edition.

Kwak, J.H., Tran, D., Burton, S.D., Szanyi, J., Lee, J.H., and Peden, C.H. (2012). Effects of hydrothermal aging on nh3-scr reaction over cu/zeolites. *Journal of Catalysis*, 287, 203–209.

Ma, Y. and Wang, J. (2020). Sliding-mode control of automotive selective catalytic reduction systems with state estimation. *Proceedings of the Institution of Mechanical Engineers, Part D: Journal of Automobile Engineering*, 234(2-3), 630–644.

Nebergall, J., Hagen, E., and Owen, J. (2005). Selective catalytic reduction on-board diagnostics: Past and future challenges. Technical report, SAE Technical Paper.

Papageorgiou, D., Blanke, M., Niemann, H.H., and Richter, J.H. (2018). Robust backlash estimation for industrial drive-train systems-theory and validation. *IEEE Transactions on Control Systems Technology*, 27(5), 1847–1861.

Schär, C.M. (2003). *Control of a selective catalytic reduction process*. ETH Zurich.

Skaf, Z., Aliyev, T., Shead, L., and Steffen, T. (2014). *The state of the art in selective catalytic reduction control*. SAE International.

Song, Q. and Zhu, G. (2002). Model-based closed-loop control of urea scr exhaust aftertreatment system for diesel engine. *SAE Transactions*, 102–110.

Willems, F., Cloudt, R., Van Den Eijnden, E., Van Genderen, M., Verbeek, R., De Jager, B., Boomsma, W., and Van Den Heuvel, I. (2007). Is closed-loop scr control required to meet future emission targets? *SAE technical paper*, 1, 600–602.

Appendix A. THE PROJECTION OPERATOR

The projection operator Proj:$\mathbb{R}^2 \to \mathbb{R}$ for a scalar parameter estimation problem is defined by (Krstic et al., 1995)

$$\text{Proj}[\hat{\theta}, \tau] \triangleq \begin{cases} \tau, \ h(\hat{\theta}) < 0 \text{ or } h(\hat{\theta}) \geq 0 \ \& \ \dfrac{\partial h}{\partial \hat{\theta}} \tau \leq 0 \\ \left(1 - \left(\dfrac{\partial h}{\partial \hat{\theta}}\right)^2 h(\hat{\theta})\right) \tau, \ h(\hat{\theta}) \geq 0 \ \& \ \dfrac{\partial h}{\partial \hat{\theta}} \tau > 0 \end{cases}$$

where $h : \mathbb{R} \to \mathbb{R}$ is any convex continuously differentiable function. In essence, the projection operation modifies the estimation law $\dot{\hat{\theta}} = \tau$ such that the estimated parameter $\hat{\theta}$ always remains inside a compact set, which is defined as

$$\mathcal{P} = \left\{ \hat{\theta} \in (0,1) \mid h(\hat{\theta}) \leq 0 \right\} .$$

The function $h(\theta)$ is precisely chosen to be convex such that the set $\mathcal{P}$ is compact. An intuitive example for the case of two parameters is choosing $h(\boldsymbol{\theta}) = \frac{\theta_1^2}{a^2} + \frac{\theta_2^2}{b^2} - 1$ such that $h(\boldsymbol{\theta}) \leq 0$ implies that the parameters are inside or on the ellipse with axes a, b and centered at the origin. For this study, h has been chosen as

$$h(\hat{\theta}) \triangleq (1+\varepsilon)(2\hat{\theta} - 1)^2 - 1, \ 0 < \varepsilon \ll 1$$

so that θ is contained in the interval $(0, 1)$. The small positive parameter ε represents some slack variable for keeping $\hat{\theta}$ even further in the interval $(0, 1)$.